IEEE Access
Multidisciplinary | Rapid Review | Open Access Journal

Received December 27, 2018, accepted January 15, 2019, date of publication January 29, 2019, date of current version March 4, 2019.

Digital Object Identifier 10.1109/ACCESS.2019.2895625

Two-Stage Robust Security Constrained Unit Commitment Considering the Spatiotemporal Correlation of Uncertainty Prediction Error

ZHI ZHANG[1], YANBO CHEN[1], (Member, IEEE), JIN MA[2], XINYUAN LIU[3], AND WEIRU WANG[3]

[1]State Key Laboratory of Alternate Electrical Power System With Renewable Energy Sources, School of Electrical and Electronic Engineering, North China Electric Power University, Beijing 102206, China
[2]School of Electrical and Information Engineering, The University of Sydney, Sydney, NSW 2006, Australia
[3]State Grid Shanxi Electric Power Research Institute, Taiyuan 4215237, China

Corresponding author: Yanbo Chen (chenyanbo@ncepu.edu.cn)

This work was supported in part by the National Natural Science Foundation of China under Grant 51777067, and in part by the project Research on Green Dispatching Technology of Shanxi Power Grid under Grant 52053017000S.

ABSTRACT Robust optimization (RO) is an important tool to solve the security-constrained unit commitment (SCUC) problem for a power system with large-scale wind power. The main disadvantage of RO is that it is overly conservative, and the conservativeness of RO can be attributed to the uncertainty set used in the formulation. This paper proposes a two-stage robust SCUC model considering the spatiotemporal correlation of the uncertainty prediction error. First, based on the historical data, a polyhedral uncertainty set that can describe the spatial-temporal correlation of uncertainties is established, and the analytical relationship between confidence probability and the uncertain set is given. Second, a two-stage robust SCUC model with the objective of minimizing the operating cost under the forecasting scenarios is proposed based on the polyhedral set. Third, the Benders decomposition method is used to solve the proposed model according to its characteristics. The simulation results on the modified IEEE-30 and IEEE-118 bus system demonstrate that the proposed method can reduce the conservativeness of RO and guarantee the security and economy of the unit commitment.

INDEX TERMS Robust optimization, power generation dispatch, SCUC, power systems, smart grids.

I. INTRODUCTION

Although the large-scale integration of wind power promotes the green development of power systems, the uncertainty of its output brings severe challenges to the dispatching and operation of power systems. In order to cope with this challenge, new optimal dispatching strategies are urgently needed in power systems. Stochastic scheduling and robust scheduling have unique advantages in dealing with uncertainties [1]–[6]. The former generally depicts the uncertainty of wind farm output by simulating scenarios [7]–[8], while the latter describes the uncertainty by using uncertainty sets [9]–[11].

Robust optimization (RO) uses closed convex sets to describe the uncertainty of parameters and solves the optimal problem under the "worst case." Therefore, the results of RO are generally conservative. The conservativeness of RO's results is directly affected by the set of uncertain parameters. Reference [12] uses the upper and lower bounds of each uncertain variable at a certain confidence level as the uncertainty set. References [3] and [11] use the box set to describe the uncertainty, which further reduces the conservativeness of the RO. Due to the linear nature of the box set, it is more widely used in the power system. References [3] and [12] propose a general modeling method for wind power uncertainty set for RO. This method considers the time smoothing effect between different periods of a single wind power plant, which reduces the conservativeness of the uncertainty sets to some extent. In [13], based on considering the time smoothing effect of the prediction error of a single wind power plant, the spatial cluster effect between wind power plants is further considered, and the uncertainty set of wind power is further compressed.

The associate editor coordinating the review of this manuscript and approving it for publication was Mouloud Denai.

The above research works have made many contributions to reduce the conservativeness of RO. However, they all assume that the prediction error among different wind power farms and the various scheduling periods are independent of each other. In fact, the prediction error of wind power output is mainly caused by the difficulty in accurately predicting the meteorological conditions. Considering the continuity of the scheduling period and the geographical proximity of wind farms, this assumption of independence may not be guaranteed in practice and the effectiveness of the data needs to be assessed through actual data. Taking the wind power dispatching problem as an example, the wind farms not far from each other often have the correlated outputs [14]–[16].

Using the wind power data of Irish wind farms, [17] points out that the wind power prediction error sequence has autocorrelation, and proposes a statistical method to reduce the wind power prediction error by using this feature. In [18], the covariance matrix of wind power prediction error is added to the Gaussian distribution, and the model considering correlation is used to improve the economics of the robust optimal power flow model. The ellipsoidal set can consider the spatiotemporal correlation of wind power [4], and the coefficient matrix of the ellipsoid set is the covariance matrix of wind power, which has a natural advantage in incorporating the wind power correlation into the analysis. However, the mathematical form of the ellipsoid set makes it difficult to be applied to the RO problem, which limits its application.

In this paper, a two-stage robust SCUC method that takes into account the spatiotemporal correlation of uncertainty prediction error is proposed. The main contributions of this paper are twofold: (1) A linear polyhedral uncertain set that can describe the temporal-spatial correlation of uncertainty is established and sequentially integrated into the RO problem; (2) a two-stage robust SCUC model is established to minimize the operating costs robustly under uncertainties.

The rest of this paper is organized as follows: an uncertain set considering spatiotemporal correlations of the prediction error is established in Section II; the proposed two-stage robust SCUC model is then formulated in Section III; and the solution methodology is given in Section IV; Section IV presents numerical case study results, and the conclusions are drawn in Section V.

II. UNCERTAIN SET MODELING CONSIDERING SPATIOTEMPORAL CORRELATION OF PREDICTION ERRORS

In the unit commitment problem of power systems, the forecast value of wind power output and load are both uncertain quantities. This section uses wind power output as an example to construct an uncertain set considering the correlation of time and space. The uncertainty of the load can be modeled in a similar manner.

A. VERIFY THE SPATIOTEMPORAL COEEELATION OF PREDICTION ERRORS

Wind power prediction error are mainly due to complex meteorological conditions that cannot be accurately predicted. Considering the continuity of the scheduling period and the proximity of the geographic locations of the wind farms, there is a certain spatiotemporal correlation between the prediction error of adjacent time segments or adjacent wind farms. This correlation reflects the fluctuation level of wind power output and affects the conservativeness of the uncertain set of wind power.

The historical data of wind power output from October 2017 to September 2018 provided by the Belgian transmission system operator Elia [19] is used as statistical data to analyze the correlation of predicted error. In order to visually analyze the characteristics of wind power output prediction error, figure 1 shows the prediction error distribution of the statistical data of two adjacent time periods, indicating that the prediction error has a very obvious aggregation effect.

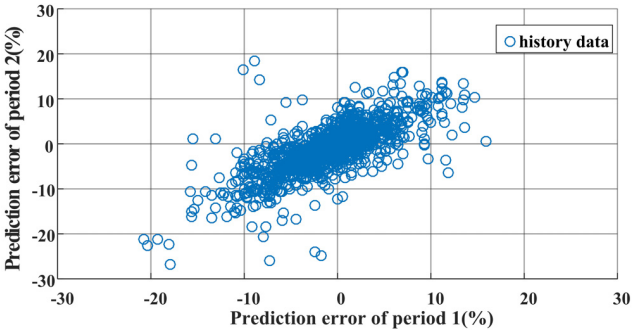

FIGURE 1. Aggregation effect of wind power measurement prediction error.

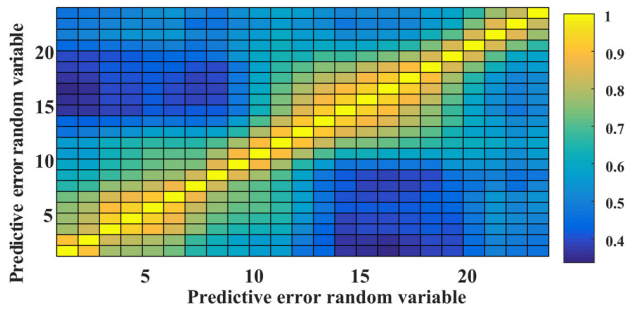

FIGURE 2. Wind power prediction error correlation matrix of different time periods of single wind farm.

Figure 2 shows the correlation coefficient matrix of the prediction error for 24 periods. In Figure 2, the horizontal and vertical coordinates respectively correspond to random vectors of prediction errors in all scheduling periods. Each square represents the prediction error correlation coefficient of the corresponding two periods. The analysis shows that the correlation coefficient of the prediction error of each

scheduling period is mostly between 0.2∼1.0, and the closer the scheduling period is, the stronger the correlation is. Therefore, there is a strong correlation between prediction errors of adjacent scheduling periods.

In addition to the strong temporal correlations among the wind power predication error, there also exist the strong spatial correlations among them, which proved in figure 9 of section V.

B. OVERVIEW OF TYPICAL UNCERTAIN SETS

In [10]–[12], the modeling problem of uncertainty set of wind power output is studied. W_1 represents the upper and lower bounds of wind power output. The main idea is to consider the time smoothing effect W_2 and spatial cluster effect W_3 of wind power output in the confidence interval. This method is called box-type uncertain set (BUS) modeling, and its mathematical model can be briefly expressed as follows

$$W^{BUS} = W_1 \cap W_2 \cap W_3 \tag{1}$$

$$W_1 = \{w_{wt} | w^e_{wt} - K\sigma_{wt} \le w_{wt} \le w^e_{wt} + K\sigma_{wt} \forall i \in G_w, \forall t \in T\} \tag{2}$$

$$W_2 = \left\{ w_{wt} | \sum\nolimits_{t=1}^{|T|} \frac{|w_{wt} - w^e_{wt}|}{\sigma_{wt}} \le \Gamma^T_w \forall w \in G_w \right\} \tag{3}$$

$$W_3 = \left\{ w_{wt} | \sum\nolimits_{t=1}^{|G_w|} \frac{|w_{wt} - w^e_{wt}|}{\sigma_{wt}} \le \Gamma^S_t \forall t \in T \right\} \tag{4}$$

where, w_{wt} represent the actual wind power output; w^e, σ represent the expectation wind power output and the standard deviation of the prediction error, respectively; K is a constant, determined by the given confidence probability α; G_w, T are sets of wind farms and scheduling periods respectively, $|G_w|$ and |T| represent their cardinality respectively; Γ^T is a time-indeterminate budget, which is used to describe the time smoothing effect of wind power output; Γ^S is a spatially uncertain budget, which is u sed to describe the spatial clustering effect of wind power output.

The uncertain budgets in Eq. (3) and (4) can be described by expectation values and standard deviations without knowing the specific distribution. Γ^T and Γ^S can be obtained based on Chebyshev's inequality [20], which are expressed as follows

$$\begin{cases} K = \sqrt{\dfrac{1}{1-\alpha}} \\ \Gamma^T_w = \mu_{wT} + \sigma_{wT}\sqrt{\dfrac{1}{1-\alpha_T} - 1} \\ \Gamma^S_t = \mu_{tS} + \sigma_{tS}\sqrt{\dfrac{1}{1-\alpha_S} - 1} \end{cases} \tag{5}$$

where, μ_{wT} and σ_{wT} are the expected and standard deviations of $\sum_{t=1}^{|T|} \left| \frac{w_{wt} - w^e_{wt}}{\sigma_{wt}} \right|$, respectively; μ_{tS} and σ_{tS} are the expected and standard deviations of $\sum_{t=1}^{|G_w|} \left| \frac{w_{wt} - w^e_{wt}}{\sigma_{wt}} \right|$, respectively; α_T and α_S are the given confidence probabilities.

C. UNCERTAIN SET MODELING CONSIDERING SPATIOTEMPORAL CORRELATION OF PREDICTION ERRORS

Covariance is a typical parameter that characterizes the correlation of random variables. The covariance matrix of the wind power output prediction error can be obtained through the statistical analysis on historical data.

Denote the covariance matrix of the wind power vector $\boldsymbol{w}$ as $\boldsymbol{\Sigma}$. The wind power output vector can be represented by

$$\boldsymbol{w} = \boldsymbol{w}^e + \Delta\boldsymbol{w} \tag{6}$$

where, $\boldsymbol{w}$ is the wind power output random vector, the expectation of the random vector $\boldsymbol{w}$ is $\boldsymbol{w^e}$; $\Delta\boldsymbol{w}$ is the wind power prediction error vector. According to the statistical data, the expectation $E(\Delta\boldsymbol{w}) = \boldsymbol{0}$ of $\Delta\boldsymbol{w}$, and the covariance is $cov(\Delta\boldsymbol{w}) = \boldsymbol{\Sigma}$. $\Delta\boldsymbol{w}$ can also be expressed as [21]

$$\Delta\boldsymbol{w} = \boldsymbol{\Sigma}^{1/2}\boldsymbol{v} \tag{7}$$

where, $\boldsymbol{v}$ is a random vector, which is expected to be $\boldsymbol{0}$, and the covariance matrix is an identity matrix.

Multiplying both sides of Eq.(7) by $\boldsymbol{\Sigma}^{-1/2}$, we have

$$\boldsymbol{v} = \begin{bmatrix} v_1 \\ \vdots \\ v_n \end{bmatrix} = \boldsymbol{\Sigma}^{-1/2}\Delta\boldsymbol{w} = \boldsymbol{\Sigma}^{-1/2} \begin{bmatrix} \Delta w_1 \\ \vdots \\ \Delta w_n \end{bmatrix} \tag{8}$$

In the formula, each random variable of $\boldsymbol{v}$ is independent of each other, and when a distribution of $\boldsymbol{v}$ is given, the distribution forms of $\Delta\boldsymbol{w}$ and $\boldsymbol{w}$ can be indirectly determined.

1) ELLIPSOID UNCERTAINTY SET

Given the distribution of $\boldsymbol{v}$, the distribution of $||\boldsymbol{v}||_2$ can be obtained from Eq. (9).

$$\|\boldsymbol{v}\|_2 = \boldsymbol{v}^T\boldsymbol{v} = \Delta\boldsymbol{w}^T\boldsymbol{\Sigma}^{-1}\Delta\boldsymbol{w} = v_1^2 + v_2^2 + \cdots v_n^2 \tag{9}$$

In particular, when v_w obeys a standard normal distribution, $\|\boldsymbol{v}\|_2$ obeys the chi-square distribution with a freedom degree n, i.e. $\sum v_w^2 \sim \chi^2(n)$ [22].

Apply Eq.(6) to the uncertainty modeling of wind power output, $\boldsymbol{w^e}$ denotes the expected value vector of wind power output, $\Delta\boldsymbol{w}$ denotes the wind power output prediction error vector. the uncertainty set of wind power output can be expressed as

$$\boldsymbol{W}^{EGF} = \left\{ \boldsymbol{w}^e + \Delta\boldsymbol{w} | \Delta\boldsymbol{w}^T\boldsymbol{\Sigma}^{-1}\Delta\boldsymbol{w} \le K_\alpha \right\} \tag{10}$$

In the formula, K_α is a constant corresponding to the cumulative probability distribution of $\chi^2(n)$ when the confidence probability is equal to α.

The distribution of $\boldsymbol{v}$ in Eq.(9) can be obtained by analyzing the actual output characteristics of wind power. The fact that wind power prediction error approximately satisfies certain distribution characteristics has been widely confirmed and recognized [18]. Figure 3 shows the distribution of the measured wind power prediction error data of Elia. As can be seen from figure 3, the distribution of the wind power prediction error can be approximated by the normal distribution. Since $\boldsymbol{v}$

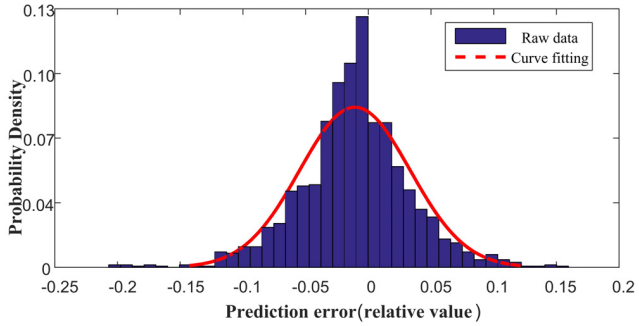

FIGURE 3. Schematic diagram of normal distribution of Elia prediction error original data.

is a random vector, which expectation is $\mathbf{0}$, and the covariance matrix is an identity matrix, so the random variables v_w in $\boldsymbol{v}$obey the standard normal distribution.

In order to facilitate the subsequent comparative analysis, when the wind power prediction error obeys the normal distribution, the wind power output uncertainty set given by Eq.(10) is recorded as the ellipsoid uncertainty set (EUS). In the next section, the ellipsoidal forms are converted to the polyhedral uncertain sets to reflect the temporal-spatial correlations of prediction error.

2) POLYHEDRAL UNCERTAINTY SETS

Considering that random variables $v_w(w = 1, 2, \cdots, n)$ in Eq. (8) are independent of each other, defining the distribution of v_w respectively can also indirectly determine the distribution of $\Delta \boldsymbol{w}$ and $\boldsymbol{w}$. Give a confidence probability α, and assume that $v_1, v_2, \cdots, v_n$ has the same confidence probability β, then we have $\beta_w = \alpha, w = 1, \cdots, n$. The probability that the random vector $\Delta \boldsymbol{w}$ satisfies the following inequality is α [20], [21].

$$-\boldsymbol{U}^{\beta} \leq \begin{bmatrix} v_1 \\ \vdots \\ v_n \end{bmatrix} = \boldsymbol{\Sigma}^{-1/2} \begin{bmatrix} \Delta w_1 \\ \vdots \\ \Delta w_n \end{bmatrix} \leq \boldsymbol{U}^{\beta} \tag{11}$$

where, $\boldsymbol{U}^{\beta} = \left[U_1^{\beta}, \cdots, U_w^{\beta}, \cdots, U_n^{\beta}\right]^T$, U^{β} is a constant corresponding to the cumulative distribution of the random variable v_w when the confidence probability is equal to β.

The wind power output uncertainty set is then given by

$$\boldsymbol{W}^{PGF} = \left\{ \boldsymbol{w}^e + \Delta \boldsymbol{w} | - \boldsymbol{U}^{\beta} \leq \boldsymbol{\Sigma}^{-1/2} \Delta \boldsymbol{w} \leq \boldsymbol{U}^{\beta} \right\} \tag{12}$$

The wind power uncertainty set of Eq. (12) shows that the weighted wind power predication errors are bounded by $-\boldsymbol{U}^{\beta}$ and $\boldsymbol{U}^{\beta}$, thus the uncertainty is constrained by the polyhedral regions. For convenience of comparison, the above method was recorded as polyhedral uncertainty set (PUS).

The methods presented above control the conservativeness of the set by constructing an analytical relationship between the uncertain set of wind power output and the confidence probability. In the above method, any two random variables Δw_1 and Δw_2 of $\Delta \boldsymbol{w}$ may be prediction errors of different wind farms in the same time period, or prediction errors of different time periods of the same wind farm, which does not affect the generality and applicability of the method. For the case of $|G_w|$ wind farms with $|T|$ scheduling periods, $\Delta \boldsymbol{w}$ can be expressed as

$$\begin{aligned} \Delta \boldsymbol{w} = [&\Delta w_{1,1}, \cdots \Delta w_{1,|T|}, \cdots, \Delta w_{w,1}, \cdots, \Delta w_{1,|T|}, \cdots, \\ &\times \Delta w_{|G_w|,1}, \cdots, \Delta w_{|G_w|,|T|}] \end{aligned} \tag{13}$$

III. PROPOSED TWO-STAGE ROBUST SCUC MODEL

A. DETERMINISTIC SCUC MODEL

1) THE OBJECTIVE FUNCTION

The objective of deterministic SCUC is (14). Prevailing constraints include system power balance (20), generation capacity limits of thermal units (21)-(23) and wind farms (24), minimum on/off time limits (25)-(26), startup/ shutdown costs (27)-(28), ramping up/down limits (29)-(30), and network security constraint (31).

$$\underset{P_{it}^b, I_{it}^b, P_{wt}^b}{Min} \quad \sum_t \sum_i [C_i(P_{it}^b) + SU_{it}^b + SD_{it}^b] \tag{14}$$

$$\sum_i P_{it}^b + \sum_w P_{wt}^b = \sum_d P_{dt}^b \tag{15}$$

$$P_i^{\min} \cdot I_{it}^b \leq P_{it}^b \leq P_i^{\max} \cdot I_{it}^b \tag{16}$$

$$0 \leq P_{wt}^b \leq P_{f,wt}^b \tag{17}$$

$$\left[X_{on,i(t-1)}^b - T_{on,i}\right] \cdot \left[I_{i(t-1)}^b - I_{it}^b\right] \geq 0 \tag{18}$$

$$\left[X_{off,i(t-1)}^b - T_{off,i}\right] \cdot \left[I_{it}^b - I_{i(t-1)}^b\right] \geq 0 \tag{19}$$

$$SU_{it}^b \geq su_i \cdot (I_{it}^b - I_{i(t-1)}^b), \mathrm{SU}_{it}^b \geq 0 \tag{20}$$

$$SD_{it}^b \geq sd_i \cdot (I_{i(t-1)}^b - I_{it}^b), \mathrm{SD}_{it}^b \geq 0 \tag{21}$$

$$\begin{aligned} P_{it}^b - P_{i(t-1)}^b \leq &UR_i \cdot I_{i(t-1)}^b + P_i^{\min} \\ &\cdot (I_{it}^b - I_{i(t-1)}^b) + P_i^{\max} \cdot (1 - I_{it}^b) \end{aligned} \tag{22}$$

$$\begin{aligned} P_{i(t-1)}^b - P_{it}^b \leq &DR_i \cdot I_{it}^b + P_i^{\min} \cdot (I_{i(t-1)}^b - I_{it}^b) \\ &+ P_i^{\max} \cdot (1 - I_{i(t-1)}^b) \end{aligned} \tag{23}$$

$$\begin{aligned} &\left| \sum_m SF_{l,m} \left(\sum_{i \in U(m)} P_{it}^b + \sum_{w \in W(m)} P_{wt}^b - \sum_{d \in D(m)} P_{dt}^b \right) \right| \\ &\leq PL_l^{\max} \end{aligned} \tag{24}$$

where, P_{it}^b and I_{it}^b are the decision variables, which are the output of the generator set and the start and stop state respectively; $C_i(P_{it}^b)$ is the energy cost; SU_{it}^b and SD_{it}^b are the on-off costs; P_{wt}^b denotes the dispatch of wind farm w at time t; P_{dt}^b is the load forecast of load d at time t; $P_i^{\max}$ and $P_i^{\min}$ denote the upper and lower limits of the output of unit i; w_{wt}^e denotes the predicted value of wind power; $X_{on,it}^b$, $X_{off,it}^b$ denote the on/off time counters of unit i at time t; $T_{on,i}$, $T_{off,i}$ denote the minimum start-up and downtime limit; su_i, sd_i is the start-stop cost of unit i; UR_i, DR_i are the unit climbing power limit; $PL_l^{\max}$ denotes the maximum power flow constraint of the line; $SF_{l,m}$ denotes the node power transfer factor; $D(m)$ denotes the set of load demands located

at bus m; $U(m)$ denotes the set of thermal units located at bus m; $W(m)$ denotes the set of wind farms located at bus m.

B. ROBUST SCUC MODEL

Forecast values on system load demands P_{dt}^{b} and wind generations w_{wt}^{e} in the deterministic *SCUC* model (14)–(24) could be inaccurate. The uncertainty set for predicting the output of wind power according to Eq.(12) can be expressed as

$$\boldsymbol{w}^{u} \in \left\{ \boldsymbol{w}^{e} + \Delta \boldsymbol{w} | - \boldsymbol{U}_{w}^{\beta} \leq \boldsymbol{\Sigma}_{w}^{-1/2} \Delta \boldsymbol{w} \leq \boldsymbol{U}_{w}^{\beta} \right\} \tag{25}$$

Similarly, the uncertainty set of load forecasting can be expressed as

$$\boldsymbol{P}_{d}^{u} \in \left\{ \boldsymbol{P}_{d}^{b} + \Delta \boldsymbol{P}_{d} | - \boldsymbol{U}_{d}^{\beta} \leq \boldsymbol{\Sigma}_{d}^{-1/2} \Delta \boldsymbol{P}_{d} \leq \boldsymbol{U}_{d}^{\beta} \right\} \tag{26}$$

In robust SCUC model, the objective is to minimize the total operation costs in the expected scenario (i.e. $P_{dt}^{u} = P_{dt}^{b}$, $w_{wt}^{u} = w_{wt}^{e}$). At the same time, adjust the output of the unit in uncertain scenarios to cope with the uncertainty of wind power and load. The objective function and constraints of robust SCUC problem are as follows.

1) THE OBJECTIVE FUNCTION

$$\underset{P_{dt}^{u} \in P_{d}^{PUS}, w_{wt}^{u} \in W^{PUS}, P_{it}^{b}, I_{it}^{b}, P_{wt}^{b}}{Min} \sum_{t} \sum_{i} [C_i(P_{it}^{b}) + SU_{it}^{b} + SD_{it}^{b}] \tag{27}$$

2) THE CONSTRAINTS

(1) System balance constraint can be represented as:

$$\sum_{i} P_{it}^{u}(S) + \sum_{w} P_{wt}^{u}(S) = \sum_{d} P_{dt}^{u} \tag{28}$$

where, P_{it}^{u} and P_{wt}^{u} are the adaptive dispatch adjustment of unit i and wind farm w at time t in response to uncertain intervals; P_{dt}^{u} is the uncertain load demand of load d at time t; $S = \{P_{dt}^{u}, w_{wt}^{u}\}$.

(2) The generation limits of thermal units and wind farms.

$$P_{i}^{\min} \cdot I_{it}^{b} \leq P_{it}^{u}(S) \leq P_{i}^{\max} \cdot I_{it}^{b} \tag{29}$$

$$0 \leq P_{wt}^{u}(S) \leq w_{wt}^{u} \tag{30}$$

(3) Dispatch adjustments of thermal units in response to uncertain sets are restricted by their corrective capabilities and generation dispatches in the base case.

$$-R_{i}^{down} \cdot I_{it}^{b} \leq P_{it}^{u}(S) - P_{it}^{b} \leq R_{i}^{up} \cdot I_{it}^{b} \tag{31}$$

where, R_{i}^{up} and R_{i}^{down} are the up/down corrective action limits of unit i. Corrective capabilities R_{i}^{up}, R_{i}^{down} refer to the 10-min spinning reserve capacities of generations units.

(4) Ramping up and down limits.

$$\begin{aligned} &P_{it}^{u}(S) - P_{i(t-1)}^{u}(S) \\ &\quad \leq UR_i \cdot I_{i(t-1)}^{b} + P_{i}^{\min} \cdot (I_{it}^{b} - I_{i(t-1)}^{b}) + P_{i}^{\max} \cdot (1 - I_{it}^{b}) \end{aligned} \tag{32}$$

$$\begin{aligned} &P_{i(t-1)}^{u}(S) - P_{it}^{u}(S) \\ &\quad \leq DR_i \cdot I_{it}^{b} + P_{i}^{\min} \cdot (I_{i(t-1)}^{b} - I_{it}^{b}) + P_{i}^{\max} \cdot (1 - I_{i(t-1)}^{b}) \end{aligned} \tag{33}$$

(5) Transmission network constraint

$$\left| \sum_{m} SF_{l,m} \left(\sum_{i \in U(m)}^{P_{it}^{u}(S)} + \sum_{w \in W(m)} P_{wt}^{u}(\boldsymbol{S}) - \sum_{d \in D(m)} P_{dt}^{u} \right) \right| \leq PL_{l}^{\max} \tag{34}$$

For the sake of discussion, the compact matrix formulation (35) is used to represent the above robust SCUC model. In (35), matrix inequality (a) represents constraints in base scenario, and matrix inequality (b) represents constraints in uncertain scenarios;

$$\begin{aligned} &\underset{\boldsymbol{I}^{b}, \boldsymbol{P}^{b}}{Min} \ \boldsymbol{N}^{T} \cdot \boldsymbol{I}^{b} + \boldsymbol{c}^{T} \cdot \boldsymbol{P}^{b} \\ &s.t. \begin{cases} \boldsymbol{X} \cdot \boldsymbol{I}^{b} + \boldsymbol{Y} \cdot \boldsymbol{P}^{b} \leq \boldsymbol{g}^{b}(a) \\ \boldsymbol{Q} \cdot \boldsymbol{I}^{b} + \boldsymbol{W} \cdot \boldsymbol{P}^{b} + \boldsymbol{R} \cdot \boldsymbol{P}^{u}(S) \leq \boldsymbol{g}^{u}(S) \ (b) \\ \boldsymbol{P}^{b} \geq 0, \boldsymbol{P}^{u} \geq 0, \boldsymbol{I}^{b} \in \{0, 1\}(c) \end{cases} \end{aligned} \tag{35}$$

where, $\boldsymbol{I}^{b}$ represents commitment related decisions I_{it}^{b}, SU_{it}^{b} and SD_{it}^{b}; $\boldsymbol{P}^{b}$ represent dispatch related decisions P_{it}^{b} and P_{wt}^{b}; $\boldsymbol{P}^{u}(S)$ represents dispatch related decisions P_{it}^{u} and P_{wt}^{u} in response to uncertainties.

IV. SOLUTION METHODOLOGY

The proposed two-stage robust SCUC model (35) is solved by the Benders decomposition (BD) method, which decomposes the original model into a master UC problem and security check subproblem under various uncertainties.

A. MASTER UNIT COMMITMENT PROBLEM

The Master *UC* problem (36) derives the unit commitment $\boldsymbol{I}^{b}$ and dispatch $\boldsymbol{P}^{b}$ in the base case. The constraints include (15)-(24) and all Benders cuts obtained.

$$\begin{aligned} &\underset{\boldsymbol{I}^{b}, \boldsymbol{P}^{b}}{Min} \ \boldsymbol{N}^{T} \cdot \boldsymbol{I}^{b} + \boldsymbol{c}^{T} \cdot \boldsymbol{P}^{b} \\ &s.t. \begin{cases} \boldsymbol{X} \cdot \boldsymbol{I}^{b} + \boldsymbol{Y} \cdot \boldsymbol{P}^{b} \leq \boldsymbol{g}^{b} \\ \textit{All Benders cuts obtained so far} \\ \boldsymbol{P}^{b} \geq 0, \boldsymbol{I}^{b} \in \{0, 1\} \end{cases} \end{aligned} \tag{36}$$

B. SECURITY EVALUATION FOR UNCERTAINTY SETS

1) IDENTIFY THE WORST SCENARIOS WITH THE LARGEST SECURITY VIOLATION

The first step identifies the worst uncertainty scenario. The problem can be represented as a max-min problem given in (37).

$$\begin{aligned} &\underset{S}{Max} \underset{\boldsymbol{P}^{u}, \boldsymbol{v}}{Min} \ \boldsymbol{1}^{T} \cdot \boldsymbol{v} \\ &s.t. \begin{cases} s.t. \boldsymbol{R} \cdot \boldsymbol{P}^{u} + \boldsymbol{v} \leq \boldsymbol{g}^{u}(S) - \boldsymbol{Q} \cdot \hat{\boldsymbol{I}}^{b} - \boldsymbol{W} \cdot \hat{\boldsymbol{P}}^{b} \\ \boldsymbol{v} \geq \boldsymbol{0}, \boldsymbol{P}^{u} \geq 0 \end{cases} \end{aligned} \tag{37}$$

where, $\boldsymbol{v}$ is a vector of slack variables.

In this paper, KKT algorithm is adopted to solve (37) with integer variables in the inner minimization problem. The KKT algorithm is described as follows.

Step 1: The inner minimization problem is an LP problem, and KKT conditions can be used to transfer model (37) into a single level problem given in (38):

$$Q = Max\ \eta$$
$$s.t.\begin{cases} \eta \le \mathbf{1}^T \cdot \boldsymbol{v} \\ \boldsymbol{R}\cdot\boldsymbol{P}^u + \boldsymbol{v} \le \boldsymbol{g}^u(S) - \boldsymbol{Q}\cdot\hat{\boldsymbol{I}}^b - \boldsymbol{W}\cdot\hat{\boldsymbol{P}}^b \\ \boldsymbol{R}\cdot\boldsymbol{P}^u + \boldsymbol{v} \le \boldsymbol{g}^u(S) - \boldsymbol{Q}\cdot\hat{\boldsymbol{I}}^b - \boldsymbol{W}\cdot\hat{\boldsymbol{P}}^{bT}\cdot\boldsymbol{\lambda} \le 0 \\ \boldsymbol{\lambda} \le \mathbf{1} \\ \left[\boldsymbol{g}^u(S) - \boldsymbol{Q}\cdot\hat{\boldsymbol{I}}^b - \boldsymbol{W}\cdot\hat{\boldsymbol{P}}^b - \boldsymbol{R}\cdot\boldsymbol{P}^u - \boldsymbol{v}\right]\cdot\boldsymbol{\lambda} = 0 \\ \left[-\boldsymbol{R}^T\cdot\boldsymbol{\lambda}\right]\cdot\boldsymbol{P}^u = 0 \\ [\mathbf{1}-\boldsymbol{\lambda}]\cdot\boldsymbol{v} = 0 \\ \boldsymbol{v}\ge 0, \boldsymbol{P}^u \ge 0, S, \boldsymbol{\lambda} \le 0 \end{cases} \tag{38}$$

where, $\boldsymbol{\lambda}$ is the dual variables of (37).

Step 2: The "Big-M" method is used to solve (38) with complementarity constraints, and the worst scenario $S^{worst} = \hat{S}$ corresponding to the largest security violation can be obtained.

2) GENERATE BENDERS CUTS CORRESPONDING TO THE WORST SCENARIO WITH THE LARGEST SECURITY VIOLATION

If the largest security violation $\mathbf{1}^T \cdot \boldsymbol{v}$ in the worst scenario $\hat{S}^{worst}$ is higher than the predefined threshold (10^{-3} MWh), the security check subproblem (39) will generate feasibility Benders cut (40) corresponding to the worst scenario to the master UC problem.

$$\underset{\boldsymbol{P}^u,\boldsymbol{v}}{Min}\ \mathbf{1}^T\cdot\boldsymbol{v}$$
$$s.t.\begin{cases} \boldsymbol{R}\cdot\boldsymbol{P}^u + \boldsymbol{v} \le \boldsymbol{g}^{(u)}(\hat{S}^{worst}) - \boldsymbol{Q}\cdot\hat{\boldsymbol{I}}^b - \boldsymbol{W}\cdot\hat{\boldsymbol{P}}^b \\ \boldsymbol{v}\ge 0, \boldsymbol{P}^u \ge \mathbf{0} \end{cases} \tag{39}$$
$$\mathbf{1}^T\cdot\boldsymbol{v}\boldsymbol{C}\boldsymbol{\lambda}^T\cdot\left[\boldsymbol{Q}\cdot\left(\boldsymbol{I}^b - \hat{\boldsymbol{I}}^b\right) + \boldsymbol{W}\cdot\left(\boldsymbol{P}^b - \hat{\boldsymbol{P}}^b\right)\right] \le 0 \tag{40}$$

In summary, the solution flow of proposed two stage robust SCUC model (35) as shown in figure 4.

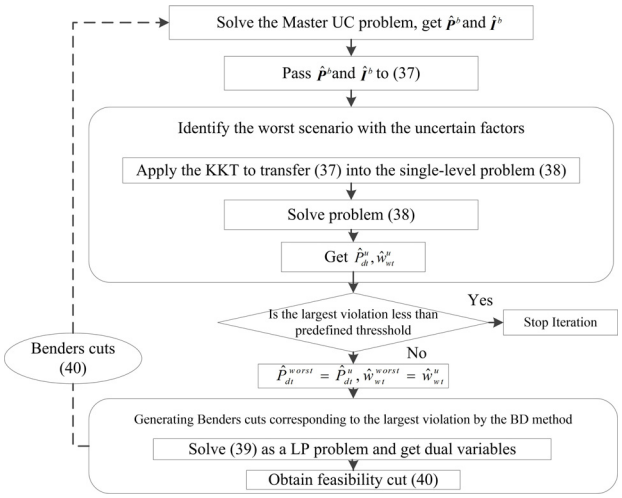

FIGURE 4. Flowchart of the proposed solution procedure.

V. CASE STUDIES

The modified IEEE-30 bus and IEEE-118 bus system are used to illustrate the effectiveness of the proposed robust SCUC approach. The two-stage robust SCUC model is solved using YALMIP and Gurobi-7.5.2 on MATLAB 2015b.

A. UNCERTAINTY SET MODELING ANALYSIS

This section evaluates the effects of wind power uncertainty set modeling using 2017.10-2018.9 historical data provided by Elia. The three uncertainty set models are evaluated by taking dispatch periods 1 and 2 of a wind farm. From Eq. (1)-(5), the BUS is mainly affected by the confidence probability α, α_T, α_S, where K is controlled by α, the time uncertainty budget Γ_T is controlled by α_T, and the spatial uncertainty budget Γ_S is controlled by α_S. This section analyzes the temporal correlation of a single wind farm, so space uncertainty budget is not considered. It can be concluded from Eq. (10) and (12) that the EUS and PUS are mainly affected by the confidence probability α.

Firstly, the influence of the confidence probability α on the uncertainty set is analyzed. α_T in the BUS is 0.9. When the given confidence probability α are 0.95, 0.9, 0.85, 0.8, the uncertainty sets constructed by the three methods of BUS, EUS and PUS are shown in figure 5.

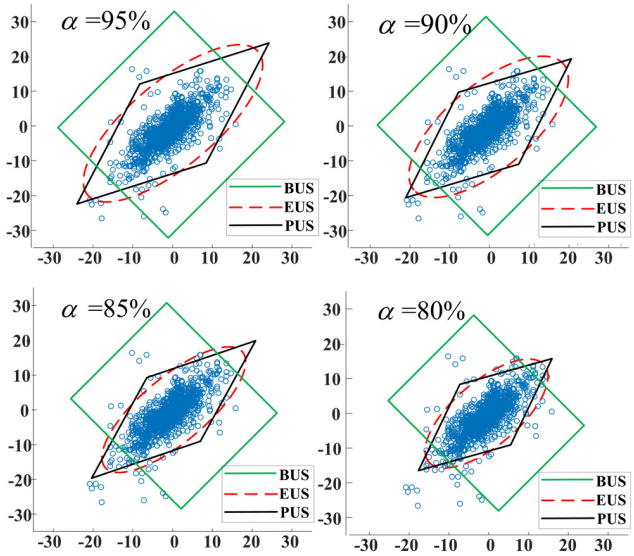

FIGURE 5. Comparison of modeling effects of three uncertain sets under different α.

It can be seen from figure 5, compared with the BUS method, the EUS and PUS methods greatly compress the space of the uncertainty set, and reduce the conservativeness

of the uncertainty set. The historical data covered by BUS, EUS and PUS models account for 98.35%, 96.15% and 95.05% respectively when α =0.95. As the confidence probability α decreases, the three uncertainty sets are compressed, the EUS and PUS are compressed on the whole, and the BUS is compressed in the direction controlled by K. The historical data covered by BUS, EUS and PUS account for 90.1%, 89.56% and 89.01% respectively when α =0.8. It can be concluded that the BUS is most affected by confidence probability α. Although the coverage of BUS is similar to EUS and PUS, but it covers a large number of ineffective area.

In addition to the influence of K, the uncertainty set BUS is also affected by the time uncertainty budget Γ_T. The Γ_T is controlled by the confidence probability α_T. α in the three uncertainty sets is 0.95. Compare the BUS, EUS and PUS when $\alpha_T = 0.95, 0.9, 0.85, 0.8$. The results shown in figure 6.

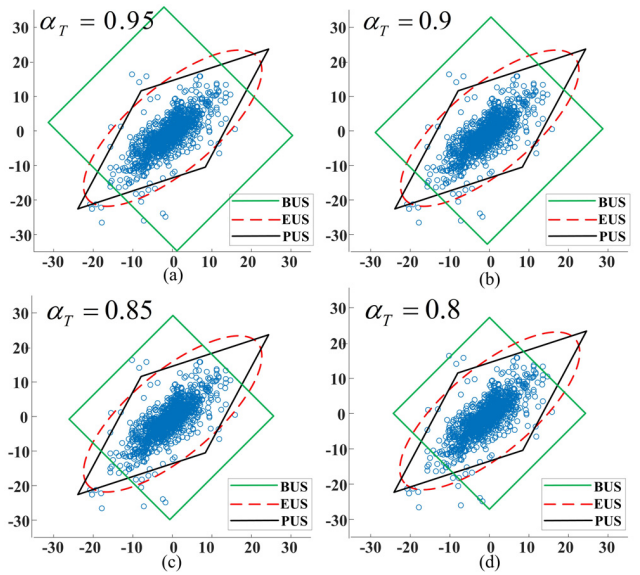

FIGURE 6. The modeling effects of BUS uncertainty set under different α_T.

As can be seen from figure 6, the EUS and PUS are not affected by the confidence probability α_T. The coverage area of the BUS varies with α_T. When $\alpha_T = 0.95, 0.9$, the boundary of the BUS controlled by K does not change. At this time, changing the confidence probability α_T can reduce the conservativeness of the uncertainty set. When $\alpha_T = 0.85, 0.8$, the size of the BUS is controlled by α_T as a whole. It can be seen from (c) and (d) in figure 6 that the conservativeness of the uncertainty set is reduced, the coverage of historical data is also decreased, resulting in the decrease in robustness. The historical data covered by BUS, EUS and PUS account for 94.50%, 96.15% and 95.05% respectively. Although the coverage of BUS is similar to EUS and PUS, but it covers a large number of ineffective areas, and its characterization accuracy is still low. At this time, the data coverage of the BUS is lower than the EUS and PUS, but its coverage area is larger than EUS and PUS. It can be concluded that the EUS and PUS can effectively reduce the conservativeness while ensuring the robustness of the uncertainty set.

B. MODIFIED IEEE-30 BUS STUDIES

The IEEE-30 bus system consists of 30 bus, 6 generators, and 41 transmission lines. Wind power and system load data are from public data from Belgian grid operator Elia. The historical data of wind power and load are scaled to meet the normal operating power range of the IEEE-30 bus system, and the BUS and PUS are constructed. The maximum load of the system is about 800MW. There is only one wind farm in the IEEE-30 node system. Therefore, this section only considers the influence of time correlation on robust scheduling. Select wind power and load forecast data for Day-ahead as the input data of the unit commitment.

In order to verify the validity of the proposed model, three unit commitment models are compared in table 1. Based on the historical data and the given confidence probability α = 0.95, the uncertain set is constructed. And given the time uncertainty budget confidence of the BUS, when α_T = 0.9, 0.85, 0.8, the uncertainty budget Γ_T is equal to 46, 40, 36, respectively. The security criterion is whether the security violation in Eq. (37) is less than a given threshold in the actual scenario of wind power and load. The three UC models as follow

TABLE 1. Comparison of scheduling results of three models.

model	α_T	solution time/s	number of iter	cost/$	Security check
SCUC	/	7.56	0	247490	not pass
RUC	0.9	192.44	8	276421	pass
	0.85	188.56	8	272884	pass
	0.8	157.04	6	266218	not pass
TRUC	/	144.96	5	258922	pass

a. Traditional security constrained unit commitment (SCUC).

b. Two-stage robust unit commitment (RUC). The BUS method is used to construct the box-type uncertain set, considering the wind power and load prediction error, but the time correlation is not considered.

c. Two-stage robust unit commitment considering the time correlation of uncertainty prediction error (TRUC).

As can be seen from Table 1, the traditional SCUC model has the lowest operating cost and the fastest calculation efficiency. However, when considering the uncertainty prediction error, the unit commitment result will not guarantee the security of the power system. Analysis of the RUC optimization results under different confidence probabilities α_T can reduce the conservativeness of the uncertainty set after considering the time uncertainty budget. When α_T = 0.8, the operating cost of the RUC model is lower than that of α_T = 0.9, but the UC decision at this time cannot guarantee sufficient robustness. It can also be seen from (d) of figure 6 that when

$\alpha_T = 0.8$, the effective area covered by the BUS is reduced. Compared with the RUC model, the TRUC model reduces the conservativeness of uncertainty set, and thereby reduces the operating cost and improves the calculation efficiency.

When considering the uncertainty, the two-stage SCUC deals with uncertainty by adjusting the unit commitment and scheduling scheme. Figure 7 shows the UC decision under different models. As can be seen from figure 6 (black represents the power-on state, white represents the shutdown state), when given the confidence probability of the uncertain set, the UC decision in base case adjusts the unit commitment to cope with the uncertainty, and the number of power-on increases, thereby resulting in an increase in economic costs. Compared with RUC (α_T =0.9), the number of startup units of TRUC is less than that of the RUC. It can be concluded that the conservativeness of the uncertainty set is limited by considering the correlation of the uncertainty prediction error.

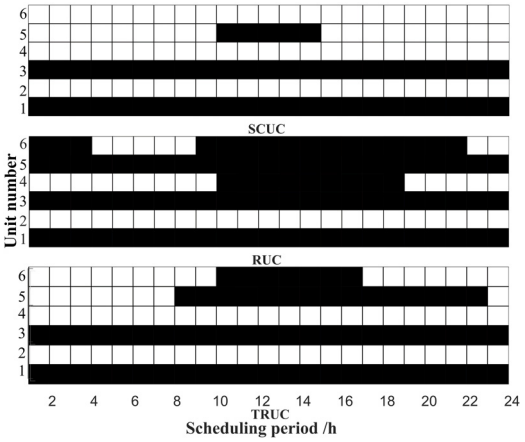

FIGURE 7. Comparison of unit combinations of the three models.

The optimization results of RUC and TRUC are mainly affected by the wind power and load uncertainty set. The conservation of TRUC method controlled by the confidence probability α. The conservation of RUC method controlled by α and α_T. The comparisons of the influence under different α, α_T on the costs of the three models are presented in figure 8.

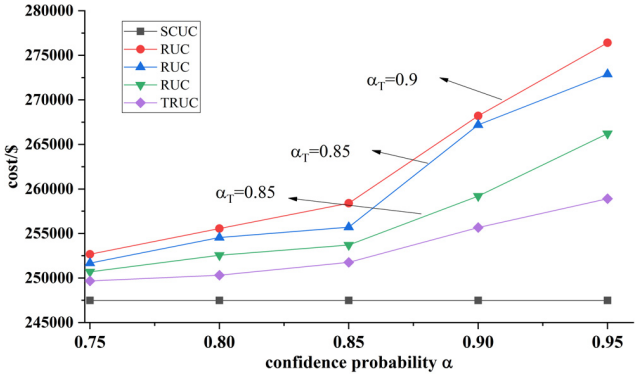

FIGURE 8. Operating costs at different confidence probabilities.

As can be seen from figure 8, the traditional SCUC model does not consider uncertainty, and its operating cost does not change with α. As the confidence probability α increases, the operating costs of the RUC and TRUC models are increased to varying degrees. Although the operating cost reduction of the RUC model with α_T reduced, the cost of RUC is always higher than that of TRUC. When the time uncertainty budget Γ_T continues to decrease with the confidence probability α_T, the robustness of the uncertainty set will be greatly reduced. So the cost of $\alpha_T < 0.8$ is no longer discussed. When the confidence probability is 75%, the operating costs of RUC and TRUC are similar to those of SCUC. This is because when the uncertainty interval is small, the system no longer needs to adjust the unit commitment plan on a large scale.

C. MODIFIED IEEE-118 BUS STUDIES

The modified IEEE-118 bus system includes 118 bus, 54 generators, 186 transmission lines, and three wind farms are installed at three buses of 17, 43, and 96. Wind power and load data are slightly adjusted to meet the normal operating power range of the IEEE-118 bus system based on Elia's published data, and wind power and load uncertainty sets are constructed from historical data. The prediction curves of load and wind power of three wind farms using the Elia data are shown in figure 9.

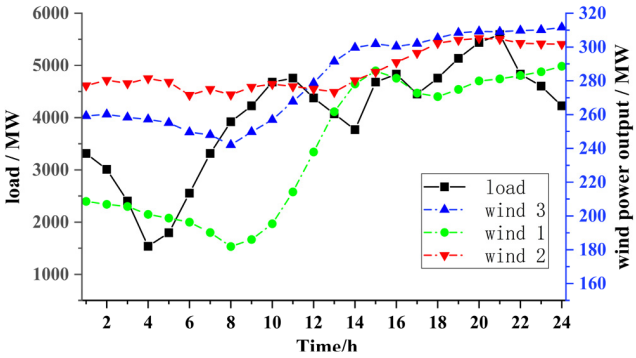

FIGURE 9. System load and wind power generation of the three wind farms.

1) ROBUST SCUC MODEL CONSIDERING THE SPATIOTEMPORAL CORRELATION

The three wind farms in the IEEE-118 bus system are spatially adjacent, so this section establishes an uncertainty set based on the spatial correlation and temporal correlation of wind power prediction errors. The robust SCUC model considering the spatiotemporal correlation of uncertainties is recorded as TSRUC. A prediction error set including 3 wind farms and 24 scheduling periods is constructed according to Eq.(13), and the standard deviation, the covariance matrix, and the correlation coefficient matrix of the prediction error set are calculated. The spatiotemporal correlation matrix of wind power prediction error is shown in figure 10. Analysis of figure 10 shows that there is a correlation between the

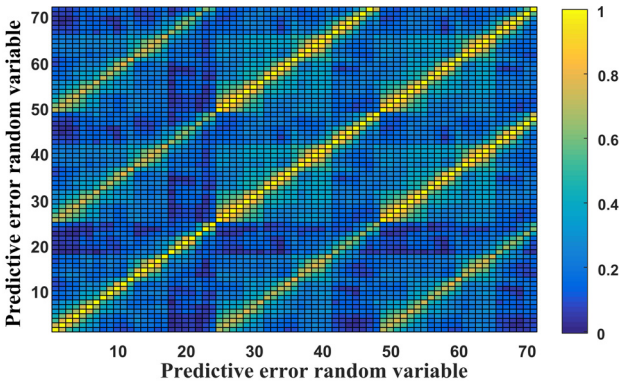

FIGURE 10. Prediction error correlation matrix.

prediction errors of different wind farms during the same time period. The prediction errors of adjacent wind farms in different time periods are also correlated, and the closer the time is, the stronger the correlation is.

The robust optimization costs comparison on SCUC, RUC, TRUC, TSRUC are shown in Table 2. In Table 2, the boundaries of the BUS, EUS, and PUS are controlled by the confidence probability α, and the confidence probability α_T, α_S respectively control the time uncertainty budget Γ_T and the spatial uncertainty budget Γ_S of the BUS.

TABLE 2. Comparison of optimization results of four models.

model	α	α_T α_S	cost/10^4 \$
SCUC	/	/	103.410
RUC	0.95	0.9	108.059
		0.85	107.447
		0.8	106.956
	0.9	0.9	106.176
		0.85	105.986
		0.8	105.302
	0.85	0.9	104.903
		0.85	104.745
		0.8	104.546
TRUC	0.95	/	106.089
	0.9	/	105.362
	0.85	/	104.720
TSRUC	0.95	/	105.642
	0.9	/	105.101
	0.85	/	104.486

As can be seen from Table 2, the SCUC model without considering uncertainty has the lowest operating cost. When considering the uncertainty, in order to cope with the worst scenario, it is necessary to adjust the UC decision, thereby resulting in an increase in operating costs. In the RUC model, comparing the operating costs under different α_T and α_S, it can be concluded that considering the time smoothing effect and the spatial clustering effect, the conservativeness of the BUS will be reduced to some extent, and the economics will be improved. The TRUC model that considers the temporal smoothing effect limits the conservativeness of uncertainty set. When considering the spatiotemporal correlation of the prediction error of multiple wind farms, the operating cost will be further reduced.

2) ROBUSTNESS TEST OF THE TSRUC MODEL

In order to verify the robustness of the proposed TSRUC model, tests are carried out for the UC decision with different confidence probabilities. The robust test is done by solving the security check subproblem for each scenario, which is restricted by unit commitment and dispatch solutions $\boldsymbol{I}^b$ and $\boldsymbol{P}^b$ in the base scenario as well as corrective capabilities in Eq.(31). The higher the ratio of the number of scenarios passed the verification to the total number of scenarios, the higher the level of robustness of the power system.

In this paper, the adjusted historical prediction error data (load and wind power) of Elia from October 2017 to September 2018 is used as input to test the robust level of the unit commitment plan with different model. The robust level test results are shown in Table 3, where α is the confidence probability of the uncertainty set, α_T, α_S are the confidence probabilities of time uncertainty budget and spatially uncertainty budget, respectively, cost denotes the robust optimization cost, OGC denotes the sum of the maximum capacity of the online unit, and α_{RO} denotes the actual robust level.

TABLE 3. Robust level test result.

Model	α	α_T α_S	cost/10^4 \$	OGC/GW	α_{RO}/%
SCUC	/	/	103.410	106.86	79.94
RUC	0.95	0.9	108.059	120.86	98.90
		0.85	107.447	118.67	98.35
		0.8	106.956	117.56	97.80
	0.9	0.9	106.176	117.11	97.52
		0.85	105.986	117.01	97.52
		0.8	105.302	113.85	96.70
	0.85	0.9	104.903	111.42	93.03
		0.85	104.745	111.10	92.85
		0.8	104.546	110.78	92.30
TSRUC	0.95	/	105.642	116.94	98.07
	0.9	/	105.101	112.67	96.97
	0.85	/	104.486	110.54	92.80

It can be seen from table 3 can conclude: 1) the larger α is, the higher the actual robustness level is, the larger the cost and OGC are. Therefore, by setting α, a reasonable lower bound of α_{RO} is given, so that a compromise between robustness and economy can be achieved by adjusting α. 2) Comparing the robustness of the RUC model with the robustness of the TSRUC model, under the same confidence probability α, when α_T, $\alpha_S = 0.9$, the robustness of the RUC model is slightly higher than TSRUC. This is because the historical data covered by the BUS uncertainty set is slightly higher than the PUS uncertainty set. At this time, the economy of the TSRUC model is significantly higher than the RUC model. This is because the uncertainty set determined by the BUS method covers a large number of invalid regions, resulting in the uncertainty set that is too conservative. By adjusting the value of α_T, α_S to change the time and space uncertainty

TABLE 4. Comparison of results of two robust scheduling models.

model	α_{set}/%	(35)/ 10^4 \$	(41)/ 10^4 \$	Difference/%
SCUC	/	103.410	103.410	0
TSRUC	95	105.642	124.937	15.4
	90	105.101	118.906	11.6
	85	104.486	115.867	9.8

budget of the BUS uncertainty set can reduce the operation cost. When α_T,$\alpha_S = 0.8$, the cost of the RUC model is close to the TSRUC model, but the robustness of the RUC model is lower than the TSRUC model. Through the above analysis, the economics and robustness of the TSRUC method is better.

3) ANALYSIS OF THE RESULTS OF THE SCUC MODEL USED IN THIS PAPER

In the power system scheduling, the general form of the classic RUC [3] is

$$\min_{\boldsymbol{x}}(\boldsymbol{c}^T\boldsymbol{x} + \max_{\boldsymbol{d}\in\boldsymbol{D}} \min_{\boldsymbol{y}\in\Omega(\boldsymbol{x},\boldsymbol{d})} \boldsymbol{b}^T\boldsymbol{y})$$
$$s.t. \begin{cases} \boldsymbol{F}\boldsymbol{x} \le \boldsymbol{f} \\ \boldsymbol{H}\boldsymbol{y} \le \boldsymbol{h} \\ \boldsymbol{A}\boldsymbol{x} + \boldsymbol{B}\boldsymbol{y} \le \boldsymbol{g} \\ \boldsymbol{I}_u\boldsymbol{y} = \boldsymbol{d} \end{cases} \tag{41}$$

The model in Eq.(41) also considers the scheduling cost in the worst scenario in the objective function, but in the power system or other engineering fields, the probability of the worst case occurring is extremely low. Therefore, it is only necessary to ensure that robust testing is feasible in the worst case. This paper establishes a two-stage robust SCUC model with the lowest operating cost in the prediction scenario as the objective function, as shown in Eq.(35). The operating cost of the two robust SCUC models are shown in table 4.

It can be seen from table 4 that the operating costs of the two models of models (35) and (41) are the same regardless of the uncertainty. When considering the uncertainty, the proposed model gives a lower cost than the classic two-stage RUC model.

4) NONANTICIPATIVE CONSTRAINT CHECK OF THE TSRUC MODEL

In the two-stage robust SCUC model considering the uncertainty of wind power output and load, the worst scenario obtained by the optimization method generally is the upper bound of load interval and the lower bound of wind power output interval. However, in practice, there may be a scenario: during the entire dispatch period, wind power and load fluctuate back and forth between the upper and lower bounds of the uncertainty interval. Due to the limit of climbing constraints, it may result in the UC decision obtained in the worst scenario is not feasible. Therefore, this paper needs to verify the feasibility in this scenario, and the verification in this scenario is called nonanticipative constraint of the robust SCUC model.

Three nonanticipative scenarios are set in this paper.

Scenario 1: The loads are the lower bound of uncertainty interval, and the wind power outputs are the upper bound of uncertainty set.

Scenario 2: The scenario 2 with maximum wind power outputs and minimum loads at odd periods, minimum wind power outputs and maximum loads at even periods.

Scenario 3: The scenario 3 with minimum wind power outputs and maximum loads at odd periods, maximum wind power outputs and minimum loads at even periods.

Based on the above three nonanticipative scenarios, the TSRUC model are verified under different confidence probability. The verification results are shown in Table 5.

TABLE 5. Nonanticipative constraint checking in three scenarios.

model	α	Scenario (1)	Scenario(2)	Scenario (3)
TSRUC	0.95	pass	pass	pass
	0.9	pass	pass	pass
	0.85	pass	pass	pass

As can be seen from Table 5, when $\alpha = 0.95$, 0.9, 0.85, the TSRUC model can operate safely under the three nonanticipative scenarios defined. Combined with figure 6, the TSRUC model considers the temporal and spatial correlation of wind power/load prediction error, and the prediction error of adjacent time or adjacent wind farm has a high correlation, so the wind power climbing and the load variation in adjacent periods are limited to a certain range. Therefore, considering the correlation of wind power output and load changes in adjacent periods can significantly reduce the need for climbing capacity of the power system. In addition, in the larger power systems, the number of units is large. There are 54 thermal units in the IEEE_118 bus system. When more units are opened in the worst scenario, the flexibility of system adjustment is higher, and it can cope with fluctuations in the output of renewable energy. Through the above analysis, it can be proved that the proposed TSRUC model can effectively deal with the nonanticipative scenarios in the uncertainty set to some extent.

VI. CONCLUSIONS

As renewable energy develops and demand response increases, the impact of various uncertainties on power system security and economic performance is critical. In this paper, a two-stage robust optimization unit commitment considering the spatiotemporal correlation of uncertainty prediction error is proposed. The method uses a polyhedral uncertain set to model the uncertain wind power and load power with spatiotemporal correlation. Based on the polyhedral model, the TSRUC model is established. Different from the RUC model in [3], the proposed robust SCUC model has established basic case scheduling and corrective measures for the uncertainty interval, which is more realistic from the engineering point of view. The case studies show that the uncertainty set considering the spatio-temporal correlation of wind/load prediction error effectively reduces the invalid

range on the basis of ensuring coverage of a large amount of historical data. Thereby reducing the conservativeness of the uncertainty set. Considering the correlation of wind power output and load in adjacent periods can significantly reduce the need for climbing capacity of the power system. Therefore, it can be concluded that the model proposed in this paper not only reduces the operating cost, but also ensures the security operation on power systems.

REFERENCES

[1] L. Wu, M. Shahidehpour, and T. Li, "Stochastic security-constrained unit commitment," *IEEE Trans. Power Syst.*, vol. 22, no. 2, pp. 800–811, May 2007.

[2] L. Wu, M. Shahidehpour, and Z. Li, "Comparison of scenario-based and interval optimization approaches to stochastic SCUC," *IEEE Trans. Power Syst.*, vol. 27, no. 2, pp. 913–921, May 2012.

[3] D. Bertsimas, E. Litvinov, X. A. Sun, J. Zhao, and T. Zheng, "Adaptive robust optimization for the security constrained unit commitment problem," *IEEE Trans. Power Syst.*, vol. 28, no. 1, pp. 52–63, Feb. 2013.

[4] B. Hu, L. Wu, and M. Marwali, "On the robust solution to SCUC with load and wind uncertainty correlations," *IEEE Trans. Power Syst.*, vol. 29, no. 6, pp. 2952–2964, Nov. 2014.

[5] R. Pinson, H. Madsen, H. A. Nielsen, G. Papaefthymiou, and B. Klöckl, "From probabilistic forecasts to statistical scenarios of short-term wind power production," *Wind Energy*, vol. 12, no. 1, pp. 51–62, Jan. 2009.

[6] A. Street, F. Oliveira, and J. M. Arroyo, "Contingency-constrained unit commitment with n-K security criterion: A robust optimization approach," *IEEE Trans. Power Syst.*, vol. 26, no. 3, pp. 1581–1590, Sep. 2011.

[7] W. Wei, F. Liu, S. Mei, and Y. Hou, "Robust energy and reserve dispatch under variable renewable generation," *IEEE Trans. Smart Grid*, vol. 6, no. 1, pp. 369–380, Jan. 2015.

[8] E. M. Constantinescu, V. M. Zavala, M. Rocklin, S. Lee, and M. Anitescu, "A computational framework for uncertainty quantification and stochastic optimization in unit commitment with wind power generation," *IEEE Trans. Power Syst.*, vol. 26, no. 1, pp. 431–441, Feb. 2011.

[9] H. Ye and Z. Li, "Robust security-constrained unit commitment and dispatch with recourse cost requirement," *IEEE Trans. Power Syst.*, vol. 31, no. 5, pp. 3527–3536, Sep. 2016.

[10] A. L. Soyster, "Technical note–convex programming with set-inclusive constraints and applications to inexact linear programming," *Oper. Res.*, vol. 21, no. 5, pp. 1154–1157, Oct. 1973.

[11] C. Zhao and Y. Guan, "Unified stochastic and robust unit commitment," *IEEE Trans. Power Syst.*, vol. 28, no. 3, pp. 3353–3361, Aug. 2013.

[12] R. Jiang, J. Wang, and Y. Guan, "Robust unit commitment with wind power and pumped storage hydro," *IEEE Trans. Power Syst.*, vol. 27, no. 2, pp. 800–810, May 2012.

[13] W. Wei, F. Liu, and S. Mei, "Game theoretical scheduling of modern power systems with large-scale wind power integration," in *Proc. IEEE Power Energy Soc. Gen. Meeting*, San Diego, CA, USA, Jul. 2012, pp. 1–6.

[14] N. Zhang, C. Kang, Q. Xia, and J. Liang, "Modeling conditional forecast error for wind power in generation scheduling," *IEEE Trans. Power Syst.*, vol. 29, no. 3, pp. 1316–1324, May 2014.

[15] J. Dupačová, N. Groewe-Kuska, and W. Roemisch, "Scenario reduction in stochastic programming: An approach using probability metrics," *Math. Program.*, vol. 95, no. 3, pp. 493–511, Jan. 2003.

[16] S. S. Soman, H. Zareipour, O. Malik, and P. Mandal, "A review of wind power and wind speed forecasting methods with different time horizons," in *Proc. North Amer. Power Symp.*, Arlington, TX, USA, Sep. 2010, pp. 1–8.

[17] G. BEL *et al.*, "Grid-scale fluctuations and forecast error in wind power," *New J. Phys.*, vol. 18, no. 2, Feb. 2016, Art. no. 023015.

[18] R. A. Jabr, "Adjustable robust OPF with renewable energy sources," *IEEE Trans. Power Syst.*, vol. 28, no. 4, pp. 4742–4751, Nov. 2013.

[19] *Belgian Grid Operator Elia Discloses Data*. Accessed: Oct. 26, 2018. [Online]. Available: http://www.elia.be/en/grid-data/

[20] G. Wang, M. Wu, and Z. Jia, *Matrix Inequality*. Beijing, China: Science Press, 2006, pp. 265–266.

[21] S. Boyd and L. Vandenberghe *Convex Optimization*, Cambridge, UK: Cambridge Univ. Press, 2004, pp. 171–172.

[22] X. Wang, *Mathematical Statistics*, Xian, China: Xi'an Jiaotong Univ. Press, 2004, pp. 17–18.

ZHI ZHANG received the B.S. degree in electrical engineering from China Three Gorges University, Yichang, Hubei, China, in 2017. He is currently pursuing the M.S. degree in electrical engineering with the School of Electrical and Electronic Engineering, North China Electric Power University. His research interests include robust modeling and optimization on power system operation.

YANBO CHEN (M'13) received the B.S. degree from the Huazhong University of Science and Technology, in 2007, the M.S. degree from the China Electric Power Research Institute, in 2010, and the Ph.D. degree from Tsinghua University, in 2013, all in electrical engineering. He is currently an Associate Professor with North China Electric Power University. His research interests include state estimation and power system analysis and control.

JIN MA received the B.S. and M.S. degrees in electrical engineering from Zhejiang University, Hangzhou, China, in 1997 and 2000, respectively, and the Ph.D. degree in electrical engineering from Tsinghua University, Beijing, China, in 2004. He is currently with the School of Electrical and Information Engineering, The University of Sydney. His research interests include load modeling, nonlinear control systems, dynamic power systems, and power system economics. He is a member of the CIGRE W.G. C4.605 Modeling and Aggregation of Loads in Flexible Power Networks and a corresponding member of the CIGRE Joint Workgroup C4-C6/CIRED Modeling and Dynamic Performance of Inverter Based Generation in Power System Transmission and Distribution Studies. He is a Registered Chartered Engineer.

XINYUAN LIU received the M.S. degree in electrical engineering from North China Electric Power University, Baoding, Hebei, China, in 2011. He is currently with the State Grid Shanxi Electric Power Research Institute, Taiyuan, China. His research interest includes power system operation, analysis, and control.

WEIRU WANG received the M.S. degree in electrical engineering from North China Electric Power University, Baoding, Hebei, China, in 2012. She is currently with the State Grid Shanxi Electric Power Research Institute, Taiyuan, China. Her research interest includes power system operation, analysis, and control.